



Geochemical Constraints on the Hydrothermal Dolomitization of the Middle-Upper Cambrian Xixiangchi Formation in the Sichuan Basin, China

Jintong Liang^{1,2,3}, Sibing Liu^{4*}, Luping Li^{1,2}, Jie Dai³, Xiaotian Li^{1,2} and Chuanlong Mou^{3*}

¹State Key Laboratory of Oil and Gas Reservoir Geology and Exploitation, Chengdu University of Technology, Chengdu, China, ²Institute of Sedimentary Geology, Chengdu University of Technology, Chengdu, China, ³Key Laboratory of Sedimentary Basin and Oil and Gas Resources, Ministry of Natural Resources, Chengdu, China, ⁴College of Energy, Chengdu University of Technology, Chengdu, China

OPEN ACCESS

Edited by:

Martyn Tranter,
Aarhus University, Denmark

Reviewed by:

Ying Bai,
Research Institute of Petroleum
Exploration and Development (RIPE),
China
Bo Jiu,
China University of Geosciences,
China

*Correspondence:

Sibing Liu
liusibing13@cdut.edu.cn
Chuanlong Mou
cdmchuanlong@163.com

Specialty section:

This article was submitted to
Geochemistry,
a section of the journal
Frontiers in Earth Science

Received: 25 April 2022

Accepted: 04 May 2022

Published: 16 June 2022

Citation:

Liang J, Liu S, Li L, Dai J, Li X and
Mou C (2022) Geochemical
Constraints on the Hydrothermal
Dolomitization of the Middle-Upper
Cambrian Xixiangchi Formation in the
Sichuan Basin, China.
Front. Earth Sci. 10:927066.
doi: 10.3389/feart.2022.927066

The Middle-Upper Cambrian Xixiangchi carbonates in the Sichuan Basin have been pervasively dolomitized. In the presented work, petrographic investigation revealed three generations of the Xixiangchi dolomites, consisting of dolomicrite (D1, 5–20 μm) with a planar-s to non-planar texture, fabric destructive dolomite (D2, 50–150 μm) with a planar-s to planar-e texture, and saddle dolomite (D3, 300 μm to 4 mm) with a planar-s to planar-e texture. D1 and D2 dolomites are presented as matrix dolomites, whereas D3 dolomites are observed as fracture-filling dolomites. Compared with the matrix D1 and D2 dolomites, which are interpreted as products of dolomitization under near-surface or at shallow burial conditions, the depleted $\delta^{13}\text{C}$ and $\delta^{18}\text{O}$ values of D3 than D1 and D2 dolomites are probably caused by the temperature-controlled isotopic fractionation within an increasing fluid–rock interaction at burial. The enriched Mn, Sr, and Ba concentrations of D3 than D1 and D2 dolomites suggest a newly introduced type of diagenetic fluids, which is probably related to the upwelling of magmatic activities (Emeishan large igneous province). By contrast, the abnormally depleted Fe concentration in D3 dolomites is attributed to its preferential incorporation into other solid phases rather than its true concentration. The similar rare earth element (REE) partition patterns of D1 and D2 dolomites demonstrate similar dolomitization fluids related to seawater or marine-origin fluids. The hydrothermal-derived D3 dolomites exhibit a different REE partition pattern by contrast. The negative Eu anomalies of D3 dolomites may represent hydrothermal fluid cooling or an association with intermediate-felsic igneous rocks. The findings of the presented work would enhance our understanding on the hydrothermal dolomitization of the Middle-Upper Cambrian Xixiangchi Formation.

Keywords: geochemical constraints, hydrothermal dolomitization, Middle-Upper Cambrian, Xixiangchi Formation, Sichuan Basin

1 INTRODUCTION

Much attention has been paid to the genesis of dolomite reservoirs over the last century because of their great hydrocarbon potential (Land, 1985; Warren, 2000; Machel, 2004; Azmy et al., 2008; Al-Aasm and Crowe, 2018; Guo et al., 2021; Kareem et al., 2021). Various models have been proposed to further understanding of the origins of dolomites, including near-surface to burial dolomitization in which multiple dolomitization events are believed to be more likely in nature rather than a single dolomitizing/diagenetic process (Al-Aasm, 2000; Azmy et al., 2001; Davies and Smith, 2006; Jiang et al., 2021). In particular, hydrothermal dolomites and associated hydrothermal dolomitization processes or hydrothermal alterations have become increasingly important in recent years (Al-Aasm et al., 2002; Machel and Lonnee, 2002; Luczaj et al., 2006; Guo et al., 2021; Li et al., 2021), since the hydrothermal dolomite reservoirs in the United States (Michigan Basin) and Canada (Appalachian Basin) have been successively proved to have the intensive potential of hydrocarbon exploration (Davies and Smith, 2006; Hollis et al., 2017).

The Middle-Upper Cambrian Xixiangchi carbonates in the Sichuan Basin have been almost entirely dolomitized and recent studies have regarded them as potential targets for further hydrocarbon exploration (Zhao et al., 2015; Hou M. C. et al., 2016a; Lei et al., 2016; Li et al., 2019). The origin and associated fluids of the Xixiangchi dolomites have also been previously investigated (Hou M. C. et al., 2016a; Yang et al., 2019), in which most dolomites formed at near-surface and mid-burial

conditions. In addition, the genetic mechanism of saddle dolomites in the Xixiangchi Formation have been examined, in which two different models were proposed including one examining their non-hydrothermal origin and association with intraformational fluids, respectively (Jiang et al., 2016; Lei et al., 2016). The current investigation is a multi-method study, including petrographic observations and geochemical analyses of matrix dolomites and fracture-filling saddle dolomites, focused on the hydrothermal dolomitization of the Xixiangchi Formation. This article aimed to 1) examine the petrographic and geochemical characteristics of the pervasive matrix dolomites and fracture-filling saddle dolomites in the Xixiangchi Formation and 2) determine the origin of their parent dolomitizing/diagenetic fluids accordingly.

2 GEOLOGICAL SETTING

The Sichuan Basin is a rhombic basin with a total area of more than 180, 000 km², lying in the western margin of the Yangtze Block (Figure 1A) in Southwest China (Li et al., 2019; Wang et al., 2008). Tectonically, the Sichuan Basin is further divided into six units, including the eastern complete fault-fold zone, the southern gentle fault-fold zone, the southwestern gentle fault-fold zone, the central flat zone, the northern gentle fault-fold zone, and the western gentle fault-fold zone (Guo et al., 1996; Zhai, 1989). The marine sediments in the Sichuan Basin cover the strata from the Sinian to the Middle Triassic age. The depositional units include the Qiongzhusi Formation, Canglangpu Formation,

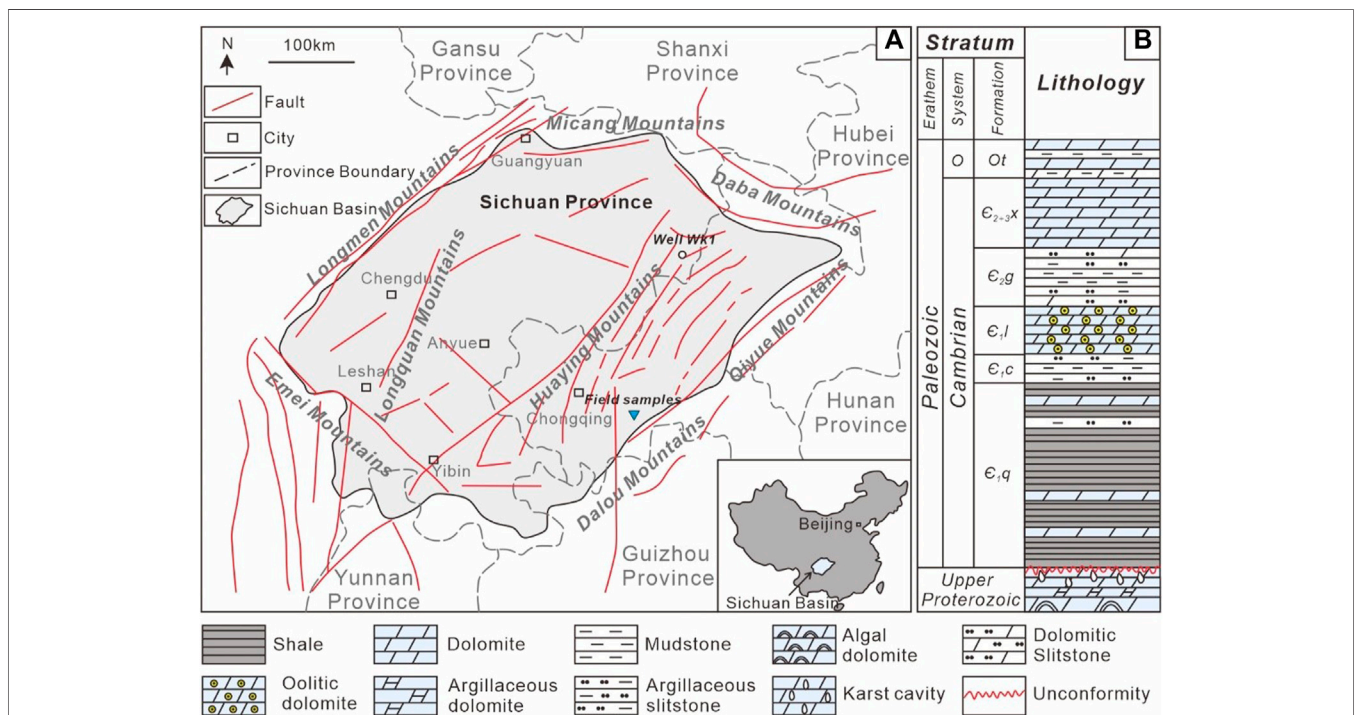


FIGURE 1 | Map of the study area showing (A) the locations of the collected field samples and drilled wells and (B) the general stratigraphic framework of the investigated Middle–Upper Cambrian Xixiangchi Formation (after Su et al., 2022).

Longwangmiao Formation, Gaotai Formation, and Xixiangchi Formation from bottom to top (**Figure 1B**). The Xixiangchi Formation was formed within a major transgression–regression cycle (Hou M. C. et al., 2016a; Jiang et al., 2016; Li et al., 2019). The Xixiangchi Formation is predominantly composed of platform carbonates, including gray to dark gray dolomicrites and crystalline dolomites with alternations of oolitic dolostone and doloarenites. In the presented reference section, the Xixiangchi Formation is dominated by massive dolostone with an occasional interaction of silty and sandy dolostone.

3 SAMPLES AND METHODS

A total of more than 70 carbonate samples were collected from the field sections in the eastern Sichuan Basin (**Figure 1**). Preliminary description and petrographic characterization were first carried out on the specimens, under which guidance, 32 dolomite samples were selected. For each sample, a set of thin-section and mirror-image slabs were polished and cleaned with deionized water for further sampling. A detailed petrographic observation was performed according to thin-section identification under a conventional polarizing microscope, which was first stained with an alizarin red S solution to differentiate the calcites from dolomites (Dickson, 1965). In addition, the thin-section identification was also carried out with the guidance of observation under a cathodoluminescope.

Microsampling was performed on slabs to extract powder samples for carbon ($\delta^{13}\text{C}$) and oxygen ($\delta^{18}\text{O}$) isotopes and major and trace elements (including rare earth elements (REEs)) testing. For stable isotopic composition, powdered samples (ca. 20 mg each) were allowed to react with 4–5 ml 100% pure phosphoric acid at 50°C to produce CO_2 . The gas product was then analyzed using a Thermo Finnigan MAT 253 isotope ratio mass spectrometer. The $\delta^{13}\text{C}$ and $\delta^{18}\text{O}$ values were reported in VPDB with analytical precisions better than $\pm 0.1\%$. For an elemental geochemical measurement, a subset of powder samples (ca. 25 mg each) was digested in a mixture of 1 ml HF and 0.5 ml HNO_3 in a Teflon beaker and reacted at 185°C for 24 h. Inductively coupled plasma mass spectrometry (ICP–MS) was used to measure Ca, Mg, Fe, Mn, Sr, and Ba, as well as REE compositions. For the REE analysis, the elemental composition was normalized to the Post-Archean Australian Shale (PAAS; McLennan, 1989) standard. A set of element anomalies, including cerium ($\text{Ce}/\text{Ce}^*_{\text{SN}} = \text{Ce}_{\text{SN}}/(0.5\text{La}_{\text{SN}} + 0.5\text{Pr}_{\text{SN}})$), europium ($\text{Eu}/\text{Eu}^*_{\text{SN}} = \text{Eu}_{\text{SN}}/(0.67\text{Sm}_{\text{SN}} + 0.33\text{Tb}_{\text{SN}})$), and lanthanum ($\text{Pr}/\text{Pr}^*_{\text{SN}} = \text{Pr}_{\text{SN}}/(0.5\text{Ce}_{\text{SN}} + 0.5\text{Nd}_{\text{SN}})$), were calculated using the equations proposed by Bau and Dulski (1965).

4 RESULTS

4.1 Petrography

The examined Xixiangchi carbonates are almost entirely dolomitized in the Sichuan Basin (Hou M. C. et al., 2016a), and the crosscut relationships suggest a possible paragenetic

sequence, as summarized in **Figure 2**. In the present work, three generations of dolomites (D1, D2, and D3) can be identified according to petrographic observations and diagenetic generations. In particular, D1 and D2 dolomites predominantly serve as the host matrix (**Figure 3**), whereas D3 dolomites are commonly observed as latter fracture-filling saddle dolomites with an occasional interaction from brecciated and fragmented matrix D1 and D2 dolomites (**Figure 3**).

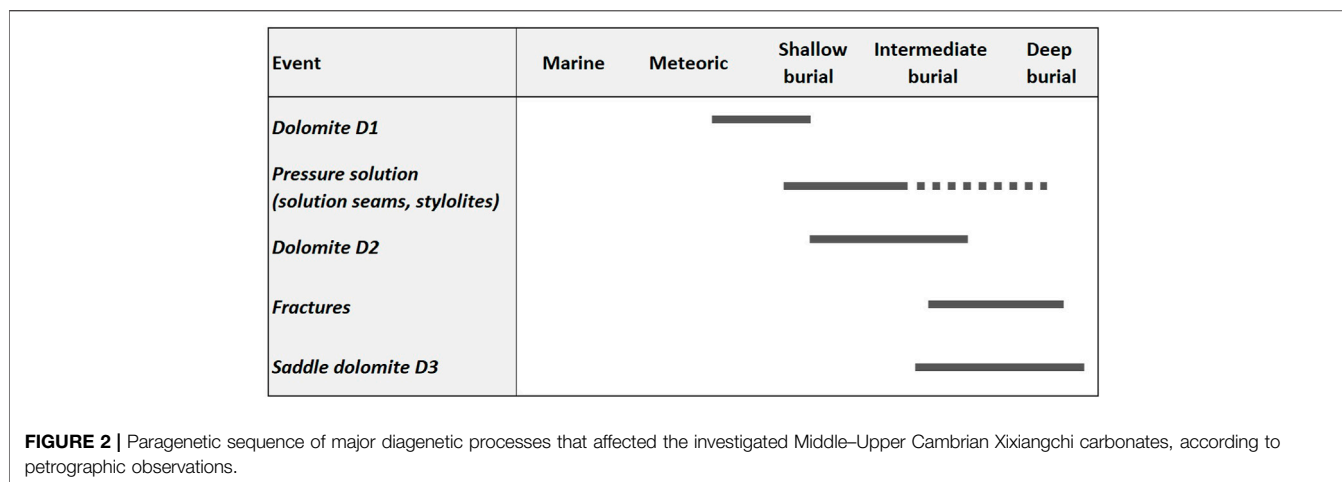
D1 dolomites (dolomicrites) predominantly consist of tightly packed micritic to near-micritic dolomites with crystal sizes ranging from 5 to 20 μm (**Figure 3A**). D1 dolomites commonly show a planar-s to non-planar texture and show dull CL under the cathodoluminescope (**Figure 3A**). The D1 generation makes up most (ca. 85%) of the studied matrix dolomites. The D2 dolomite is less abundant (ca. 15%) but has a planar-s to planar-e texture with coarser crystals (than those of D1) with a crystal size ranging from 50 to 150 μm (**Figure 3B**). Like D1, D2 dolomites exhibit dull CL under the cathodoluminescope (**Figure 3B**). D3 dolomites are fracture-filling coarser planar-s to planar-e crystals (300 μm –4 mm) with typical undulose (sweeping) extinction (**Figures 3C–F**). Unlike the matrix D1 and D2 dolomites, D3 dolomites show bright right CL features under the cathodoluminescope (**Figure 3D**). D3 dolomites are milky white in specimens (**Figure 3G**).

4.2 Carbon and Oxygen Isotopes

The stable carbon ($\delta^{13}\text{C}$) and oxygen ($\delta^{18}\text{O}$) isotopic compositions of the investigated Xixiangchi dolomites are summarized in **Supplementary Appendix Table SA1**. The average $\delta^{13}\text{C}$ and oxygen $\delta^{18}\text{O}$ values of D1 dolomites are slightly more depleted than those of D2 dolomites ($-1.5 \pm 0.2\%$ VPDB and $-9.7 \pm 0.5\%$ VPDB vs. $-1.4 \pm 0.4\%$ VPDB and $-8.9 \pm 0.7\%$ VPDB, respectively). Compared with the matrix D1 and D2 dolomites, the fracture-filling D3 dolomites have the lowest average $\delta^{13}\text{C}$ and oxygen $\delta^{18}\text{O}$ values of $-2.1 \pm 0.1\%$ VPDB and $-11.1 \pm 0.3\%$ VPDB, respectively.

4.3 Major and Trace Elements

The major and minor elemental compositions of the examined dolomites in this work are summarized in **Supplementary Appendix Table SA1**. The results of Mg and Ca concentrations imply that the presented D1, D2, and D3 dolomites are near stoichiometric and share almost the same Mg/Ca molar ratio (1.00 ± 0.04 , 0.99 ± 0.02 , and 1.01 ± 0.01 , respectively). D1 and D3 dolomites have the highest Fe concentration (2841 ± 1759 ppm) and lowest one (269 ± 83 ppm) respectively, whereas that of D2 dolomites is in the middle (1708 ± 832 ppm). By contrast, Mn concentrations show an inverse pattern; here, D3 and D1 dolomites have the highest (211 ± 42 ppm) and lowest (103 ± 44 ppm) values, respectively, while that of D2 dolomites is a moderate (147 ± 32 ppm) one. The Sr concentration decreases from 269 ± 83 ppm in D3 dolomites to 67 ± 32 ppm in D2 dolomites and drops to 60 ± 17 ppm in D1 dolomites. The Ba concentration of D2 dolomites (2.8 ± 1.3 ppm) is lower than that of D1 dolomites (6.9 ± 7.3 ppm), whereas D3 dolomites have the lowest (1.3 ± 0.4 ppm) value.



4.4 Rare Earth Elements

The composition of rare earth elements (REEs) of the investigated Xixiangchi dolomites is summarized in **Supplementary Appendix Table SA1**. The average Σ REE value of D1 dolomites is the highest (11.8 ± 6.3 ppm), whereas that of D3 dolomites is the lowest (5.6 ± 1.7 ppm). By contrast, D2 dolomites are characterized by a moderate average Σ REE value of 9.0 ± 3.8 ppm. The anomaly calculations reflect that D1, D2, and D3 almost have the same negative Ce anomalies (0.93 ± 0.04 , 0.94 ± 0.05 , and 0.95 ± 0.01 , respectively) and similar positive Pr anomalies (1.09 ± 0.02 , 1.07 ± 0.03 , and 1.09 , respectively). However, the Eu anomalies of these dolomites vary a lot, in which D1 dolomites have the lowest average value (0.65 ± 0.03), and D2 dolomites have the highest value (0.84 ± 0.05). The D3 dolomites have a moderate average Eu anomaly of 0.70 ± 0.01 falling between the D1 and D2 dolomites.

5 DISCUSSION

5.1 Origin of Dolomites

5.1.1 Dolomite Petrography

The fine crystal size, non-planar crystal boundary, and dull to dark red CL natures of the matrix D1 and D2 dolomites imply their dolomitization under near surface or at shallow burial conditions, which is consistent with the findings in the previous literature reports (Hou M. C. et al., 2016a; Jiang et al., 2016; Yang et al., 2019). This is supported by the presence of microstylolites crosscutting through D1 and D2 dolomites, which reflects limited meteoric alterations (Azmy et al., 2008; Azmy et al., 2001; Hou Y. et al., 2016b; Shembilu et al., 2021). The lack of evaporitic layers indicates dolomitization by diagenetic fluids that were likely modified by seawater rather than evaporated brines (Chow and James, 1992; Hein et al., 1992). In particular, the slightly coarser crystal size of D2 than D1 dolomites may be indicative of re-crystallization at somewhat elevated temperatures during burial diagenesis (**Figures 3A,B**). By contrast, the significant coarser crystal size and undulose

extinction of D3 dolomites that fill fractures are attributed to precipitation from hot saline brines and crystal growth at high temperatures ($>60^\circ\text{C}$) of deep burial settings (Al-Aasm et al., 2002; Shembilu et al., 2021). It is previously demonstrated that Fe and Mn elements are inhibitors and dominant activators for luminescence in carbonates, respectively (Warren, 2000; Machel, 2004). If this is the case for D3 dolomites, the variation in their CL emission intensity is likely the reflection of the documented high Mn concentrations in the vein/fracture as compared with the limited Fe concentrations (**Figure 3D**).

5.1.2 Carbon and Oxygen Isotopes

Carbon and oxygen isotopic results have been widely used to determine whether carbonates still preserve their primary signatures (Azmy et al., 2001; Hou M. C. et al., 2016a; Mahboubi et al., 2016). In the presented work, both D1 and D2 dolomites have comparable $\delta^{13}\text{C}$ values to the best-preserved Cambrian marine carbonates (-2.5 to 2.0% VPDB; Montanez et al., 2000; Veizer et al., 1999) (**Figure 4**). This resembles the Cambrian successions of the Huron Domain, Michigan Basin (Al-Aasm and Crowe, 2018), which can be reasonably inferred that the carbon isotopes have been buffered by precursor marine limestones. This means that the carbon composition of dolomitizing fluids of matrix D1 and D2 dolomites were buffered from marine carbon. By contrast, the fracture-filling D3 dolomites showed a clear negative shift from the equilibrium $\delta^{13}\text{C}$ values and presented a co-variant trend with the $\delta^{18}\text{O}$ values (**Figure 4**). This is probably caused by the temperature-controlled isotopic fractionation within an increasing fluid–rock interaction at burial (cf. Mahboubi et al., 2016; Al-Aasm and Crowe, 2018; Jiu et al., 2020; Murphy et al., 2020). Similarly, the $\delta^{18}\text{O}$ values of D1 and D2 dolomites also fall within the documented range of the best-preserved Cambrian marine carbonates (**Figure 4**), which implies that their dolomitizing fluids are probably modified by seawater (Veizer et al., 1999; Montanez et al., 2000; Shembilu et al., 2021). However, if the $\delta^{18}\text{O}$ values of dolomites in equilibrium with Cambrian seawater are adopted (Al-Aasm and Crowe, 2018), the $\delta^{18}\text{O}$ values of both D1 and D2 dolomites in the presented work show a negative shift. This

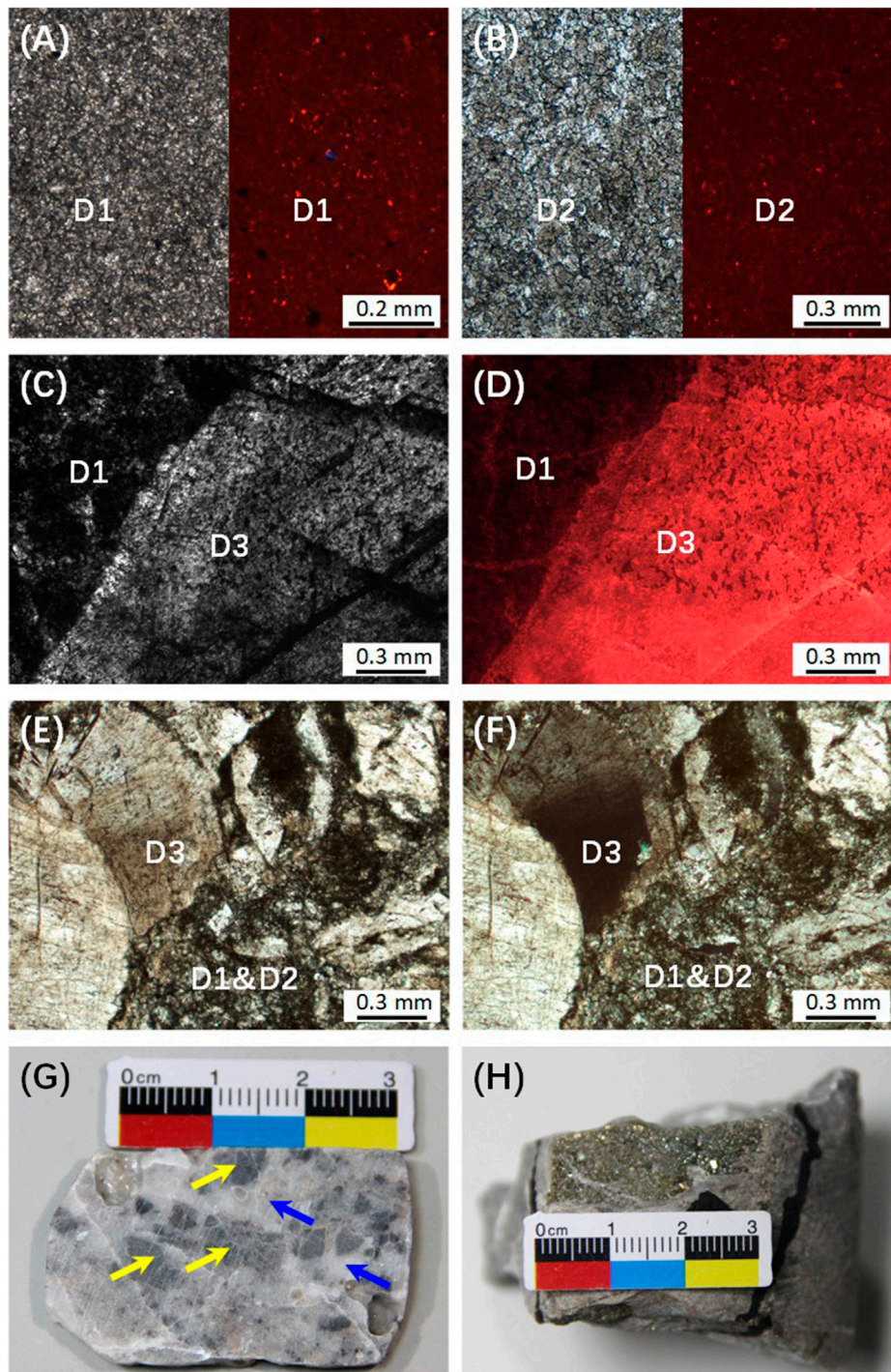
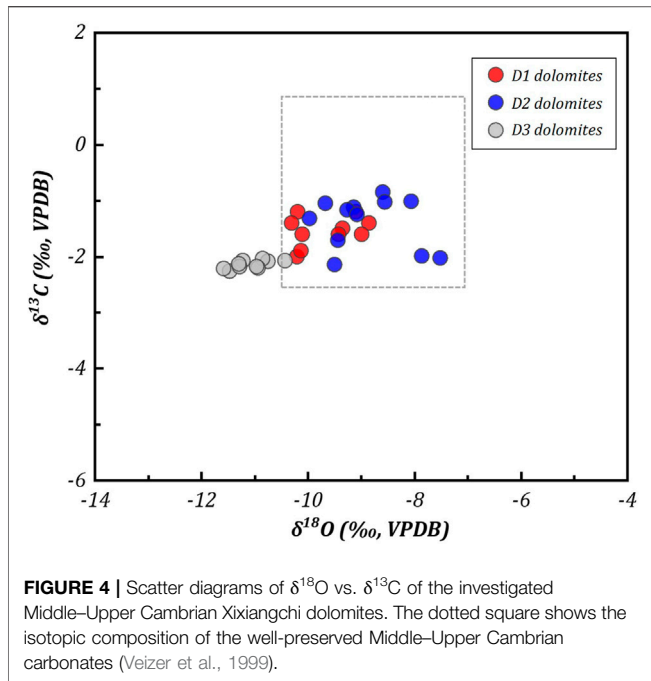


FIGURE 3 | Photomicrographs of the investigated Middle–Upper Cambrian Xixiangchi carbonates. **(A)** Fine-grained matrix D1 dolomite from sample S1, with a polarized figure on the left and a cathodoluminescence figure on the right. **(B)** Coarse-grained matrix D2 dolomite from sample S17, with a polarized figure on the left and a cathodoluminescence figure on the right. **(C)** Large-zoned D3 fracture-filling dolomite from sample S27 under polarized light. **(D)** Cathodoluminescence image of (c). D3 dolomite with undulose (sweeping) extinction under perpendicular polarized light **(F)** with the same range under plane polarized light **(E)**. **(G)** Specimen of fracture-filling D3 saddle dolomites (blue arrows) and incorporated breccias of matrix D1 and D2 dolomites (yellow arrows) from the field sample. **(H)** Core sample from well WK1 with pyrite filling the fracture (see **Figure 1** for well location).

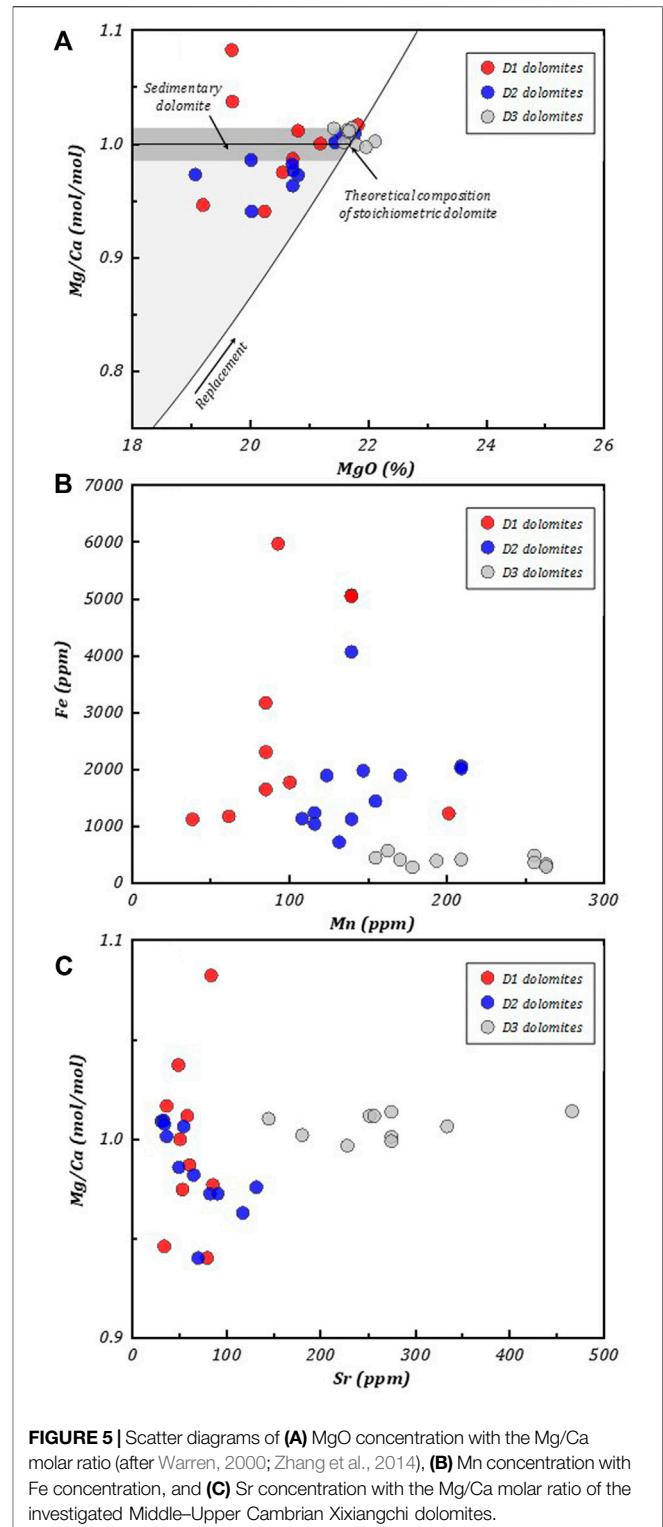


trend can be explained by the interaction with meteoric water under near-surface conditions or later alteration at elevated temperatures in burial regimes (Mahboubi et al., 2016; Al-Aasm and Crowe, 2018; Tortola et al., 2020). Considering the geological setting of the study area, the first hypothesis may be excluded due to the absence of subaerial exposures in relation to meteoric diagenesis (Al-Aasm, 2000). The latter interpretation of relatively depleted $\delta^{18}\text{O}$ values by re-crystallization with burial seems to be more likely, which corresponds well with the overlap of D1 and D2 dolomites in **Figure 4**.

5.1.3 Major and Trace Elements

5.1.3.1 Mg and Ca Concentrations

It is indicated that hypothetical sedimentary dolomites precipitate with a stoichiometric composition ($\text{CaO} = 30.4\%$, $\text{MgO} = 21.7\%$, mol (Mg/Ca) = 1; Warren, 2000). However, most of the investigated XXC dolomites showed a non-stoichiometric composition, thus indicating different fluid–rock regimes. Most of the matrix D1 and D2 dolomites had less CaO and MgO concentrations and molar ratios of Mg/Ca (**Figure 5A**; **Supplementary Appendix Table SA1**) when compared to the stoichiometric composition. This can be interpreted by the continuous dolomitizing processes in sedimentary limestones during which Mg^{2+} ions are able to replace Ca^{2+} ions (Du et al., 2018; Tortola et al., 2020). Consequently, a lower fluid–rock ratio and limited supply of Mg^{2+} ions would result in the decreased MgO and CaO concentrations in D1 and D2 dolomites, especially when other elements are incorporated into the dolomite lattices (Machel, 2004; Warren, 2000). By contrast, the fracture-filling D3 dolomites are characterized by higher MgO concentrations ($21.7 \pm 0.2\%$ on average) and a molar ratio of Mg/Ca above 1 (**Figure 5A**). This is probably due to an elevated fluid–rock interaction regime most likely found in an isotopically



open system, thus resulting in a higher molar ratio of Mg/Ca in the D3 dolomites (Brand and Veizer, 1980; Budd, 1997; Murphy et al., 2020). This interpretation fits well with the deviation of both $\delta^{18}\text{O}$ and $\delta^{13}\text{C}$ values away from those of matrix D1 and D2 dolomites, which is indicative of diagenetic alteration (**Figure 4**).

5.1.3.2 Fe and Mn Concentrations

During the dolomitizing processes, the Fe^{2+} and Mn^{2+} ions are able to replace the Ca^{2+} and Mg^{2+} ions in the dolomite lattices due to their similar radius (Azmy et al., 2008; Smith, 2006). Therefore, the concentrations of these two elements are supposed to increase with re-crystallization. In addition, their concentrations are also affected by the redox conditions in the diagenetic environment (Montanez, 1994; Veizer, 1983). In this case, dolomites formed at near-surface or shallow burial conditions seem to have less Fe and Mn concentrations than those formed in a deep burial regime (Al-Aasm, 2000; Shembilu et al., 2021). This corresponds well with the presented less Mn concentrations of the matrix D1 and D2 dolomites and its higher concentration of fracture-filling D3 dolomites in this study (Supplementary Appendix Table SA1; Figure 5B). However, this is not the case for Fe concentration in this study, in which an inverse trend of $\text{D1} > \text{D2} > \text{D3}$ is presented (Supplementary Appendix Table SA1; Figure 5B). The higher Fe concentration of D1 than D2 and D3 dolomites may be due to the incorporation of continental plastics and detrital minerals (Supplementary Appendix Table SA1). Additionally, it should be noticed that the fracture-filling D3 dolomites are unusually characterized by the highest concentration of Mn but the lowest concentration of Fe. This resembles the vein-filling saddle dolomites in the Miocene Monterey Formation, Tepusquet area (Malone and Paul, 1996), in which a low Fe concentration is attributed to its preferential incorporation into other solid phases rather than its true concentration. Such an interpretation is probably supported by the presence of pyrites in cored wells (Figure 3H) in the Sichuan Basin, even though no pyrite was observed in the investigated samples. If this is the case for D3 dolomites, such Fe and Mn concentrations would shed light on the hydrothermal origin of D3 in a reducing condition at burial.

5.1.3.3 Sr and Ba Concentrations

The decreased Sr concentration in dolomites has been previously related to the purification of dolomite during re-crystallization (Land, 1985; Malone and Paul, 1996). This is the case for matrix D1 and D2 dolomites, in which a negative correlation between Mg/Ca molar ratio and Sr concentration is roughly reflected (Figure 5C). In this process, a portion of the original Sr in D1 and D2 dolomites may have been lost when transferring into a more stoichiometric state *via* re-crystallization (Tortola et al., 2020). By contrast, no significant correlation between the Mg/Ca molar ratio and Sr concentration is obtained in the fracture-filling D3 dolomites. This is probably because D3 dolomites, with elevated Sr concentrations compared with the matrix D1 and D2 dolomites, have not undergone significant re-crystallization (Malone and Paul, 1996). Alternatively, this may be caused by a newly introduced dolomitizing fluid, such as the upwelling igneous-related brines or hot intraformational brines, for D3 which is chemically distinct from the recrystallized matrix D1 and D2 dolomites (Malone and Paul, 1996). The second interpretation is supported by higher Ba concentrations in D3 dolomites than in D1 and D2 dolomites (Supplementary Appendix Table SA1) as the Ba element is only able to be incorporated into the lattice at high temperatures (Zhang et al., 2009).

5.1.4 Rare Earth Elements

The REE signature is of great significance in determining the origin of fluids and characteristics of oceanographic processes since the diagenesis of carbonates at low fluid-rock interaction exerts limited alteration on their REE compositions (Azmy et al., 2008; Hou Y. et al., 2016b; Shembilu et al., 2021). The PAAS-normalized patterns of the REE mean values of the matrix D1 and D2 dolomites showed similar partition patterns except for Eu anomalies (Figure 6), indicating that they developed from a similar dolomitizing fluid at least. The moderate to weak negative Ce anomalies of D1 and D2 dolomites (Figure 7) likely suggested possible weak-oxidizing conditions as they are widely used as proxies for the redox conditions (Yang et al., 2018; Shembilu et al., 2021). Similarly, the Eu anomalies may also provide insights into the redox conditions; here, the negative Eu anomalies likely reflect an alkaline and oxic environment (Haas et al., 1995; Feng et al., 2016). Thus, the higher Eu anomalies of D2 than D1 may be the result of the increasing temperature of the dolomitizing fluid. By contrast, the fracture-filling D3 saddle dolomites showed different PAAS-normalized REE patterns, likely implying a different type of dolomitization fluid from the matrix D1 and D2 dolomites. In particular, the REE partition pattern of D3 dolomites is characterized by slight LREE depletion and HREE enrichment which resembles that of seawater, thus implying that the diagenetic fluids may probably be diluted by seawater (Figure 6). Although both D1 and D3 dolomites are characterized by obvious negative Eu anomalies, such behaviors may be attributed to different dolomitization fluids and diagenetic conditions. Further interpretation is made in the following chapter.

5.2 Source of Hydrothermal Fluids

It has been proved that the hydrothermal dolomite reservoirs are of great hydrocarbon potential (Guo et al., 2021; Hollis et al., 2017; Kareem et al., 2021; Li et al., 2021). Although multiple models have been already proposed to interpret the origin of ancient dolomites, it still remains controversial when it comes to the hydrothermal dolomitization and associated alterations since these processes are probably related to distinctive tectonic settings, potential fluid sources, fluid temperatures, fluid migrations, and kinetic mechanisms (Friedman, 2007; Guo et al., 2021; Hollis et al., 2017; Morad et al., 2012; Smith, 2006). Recently, the origins of hydrothermal dolomites and their associated diagenetic fluids in the Upper-Middle Cambrian dolomites in the Sichuan Basin have been extensively discussed, and two different interpretations of the formation mechanisms of saddle dolomites have been proposed. The former favors the theory that the dolomitization fluids originated from intraformational brines (Peng et al., 2018). By contrast, the latter argues for the hypomagma activity-related hydrothermal dolomitization (Lei et al., 2016). If the first interpretation is the case for the D3 dolomites in this work, the matrix D1 and D2 dolomites should show similar geochemical signatures or regular variations, such as Sr and Mn concentrations. However, such an expected phenomenon is not observed in

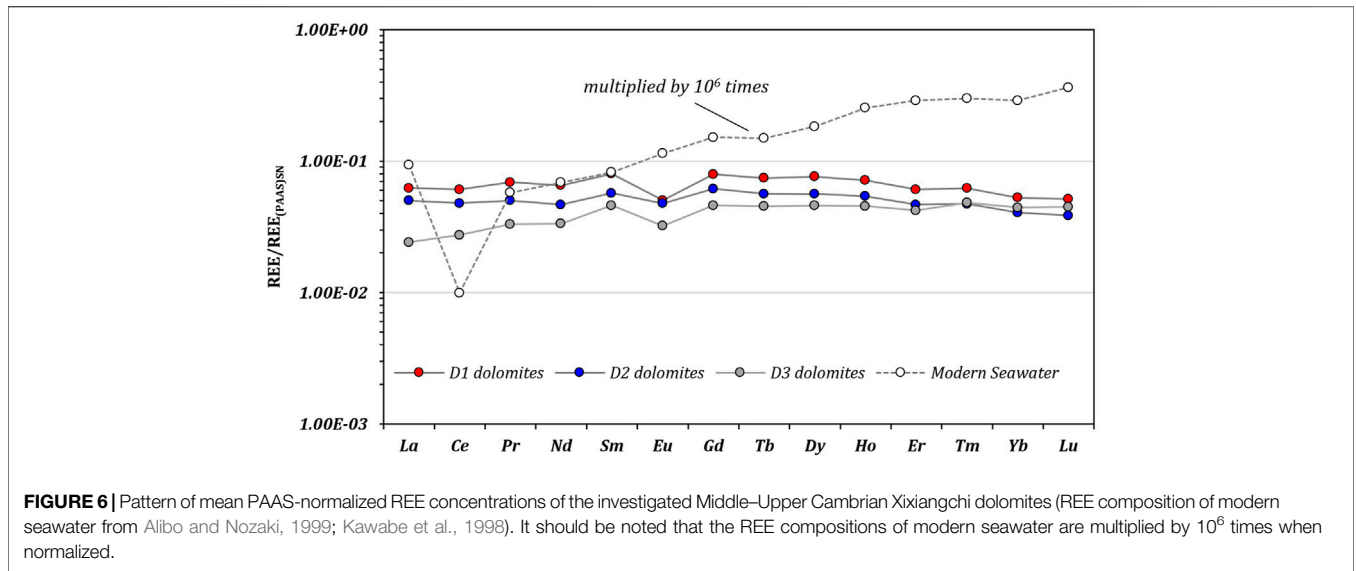


FIGURE 6 | Pattern of mean PAAS-normalized REE concentrations of the investigated Middle–Upper Cambrian Xixiangchi dolomites (REE composition of modern seawater from Alibo and Nozaki, 1999; Kawabe et al., 1998). It should be noted that the REE compositions of modern seawater are multiplied by 10^6 times when normalized.

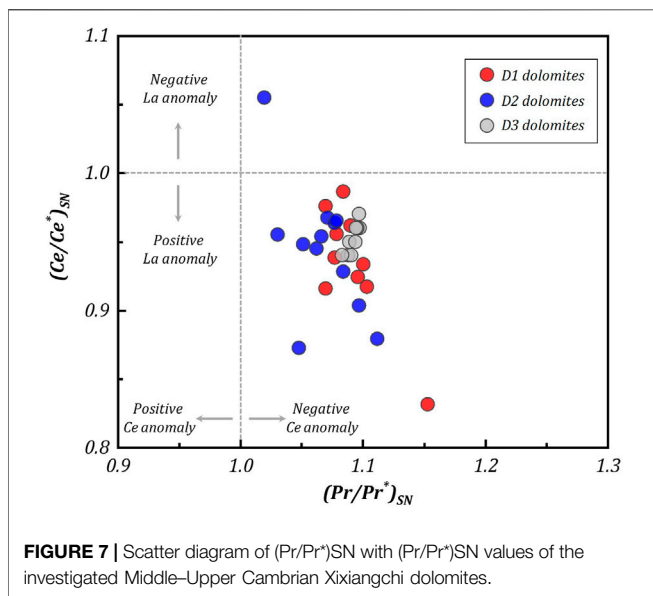


FIGURE 7 | Scatter diagram of $(Pr/Pr^*)_{SN}$ with $(Pr/Pr^*)_{SN}$ values of the investigated Middle–Upper Cambrian Xixiangchi dolomites.

the presented dolomites. In particular, if the seawater-origin brines have circulated rapidly enough to stay unaffected by the surrounding rocks and remain oxic with limited Fe concentrations (Malone and Paul, 1996), then the fracture-filling D3 dolomites should also show lower Mn concentrations rather than the observed higher concentrations (Figure 5B). Alternatively, if the diagenetic fluids for D3 dolomites share a similar origin with that of D1 and D2 dolomites, the Fe and Mn concentrations should display covariant trends at burial. Therefore, with the aforementioned depicted discrepancies, the latter explanation of a newly introduced dolomitizing fluid for D3 seems more reasonable. As such, the higher Sr and Mn concentrations of D3, compared with D1 and D2 dolomites,

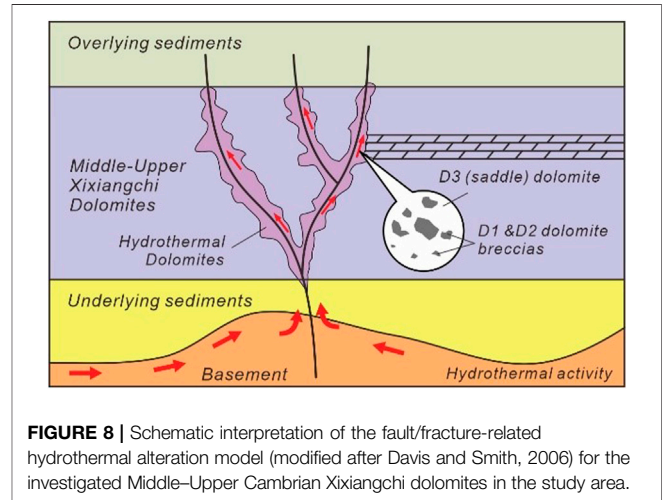


FIGURE 8 | Schematic interpretation of the fault/fracture-related hydrothermal alteration model (modified after Davis and Smith, 2006) for the investigated Middle–Upper Cambrian Xixiangchi dolomites in the study area.

are probably suggestive of a hydrothermal dolomitizing process (Zhang et al., 2009; Jiang et al., 2021).

Notably, the negative Eu anomalies (Figure 7) in the PAAS-normalized REE signature of D3 dolomites should be further discussed if a hydrothermal dolomitizing model is accepted as positive Eu anomalies have been commonly reported in saddle dolomites in relation to magmatism (Davies and Smith, 2006; Douville et al., 2002; Lei et al., 2016; Li et al., 2021). The observed negative Eu anomalies of the D3 dolomites are probably attributed to fluid-cooling since positive Eu anomalies can only develop at temperatures above 200–250°C (Bau, 1991; Jiu et al., 2020; Rieger et al., 2022). However, such signatures may be masked when the hot hydrothermal fluids were cooled below 200–250°C while circulating or mixing with seawater (Figure 8), thus resulting in negative Eu anomalies. Alternatively, such a phenomenon may be reasonably related to the upwelling of the Emeishan large igneous province (Hou M. C. et al., 2016a; Lei

et al., 2016; Li et al., 2021). In this case, the fracture-filling D3 dolomites are believed to form in association with the activity of intermediate-felsic igneous rocks (Figure 8), which may exhibit negative Eu anomalies despite their hydrothermal origins (Zhu et al., 2010; Li et al., 2020). It should be noticed that the presented interpretations mentioned previously are preliminarily made on the current database available. Additional investigations are needed to better understand the origin of hydrothermal D3 dolomites in the examined carbonate interval, such as U-Pb dating (Salih et al., 2020; Pan et al., 2021) and Mg-isotope constraining (Ning et al., 2020; Mansurbeg et al., 2021).

6 CONCLUSION

According to the petrographic observation, stable isotopic examination, and elemental composition investigation, the findings of the Middle–Upper Cambrian Xixiangchi dolomites in the Sichuan Basin are summarized as follows:

- (1) Three generations of dolomites in the Xixiangchi Formation are identified in the presented work, including dolomicrite (D1, 5–20 μm) with a planar-s to non-planar texture, fabric destructive dolomite (D2, 50–150 μm) with a planar-s to planar-e texture, and saddle dolomite (D3, 300 μm to 4 mm) with a planar-s to planar-e texture. D1 and D2 dolomites are presented as matrix dolomites, whereas D3 dolomites are observed as fracture-filling dolomites.
- (2) Compared with matrix D1 and D2 dolomites, which are interpreted as products of dolomitization under near-surface or at shallow burial conditions, the depleted $\delta^{13}\text{C}$ and $\delta^{18}\text{O}$ values of D3 than D1 and D2 dolomites are probably caused by temperature-controlled isotopic fractionation within an increasing fluid–rock interaction at burial.
- (3) The enriched Mn, Sr, and Ba concentrations of D3 than D1 and D2 dolomites suggest a newly introduced type of diagenetic fluids, which are probably related to the upwelling of magmatic activities. By contrast, the abnormally depleted Fe concentration in D3 dolomites is

attributed to its preferential incorporation into other solid phases rather than its true concentration.

- (4) The similar REE partition patterns of D1 and D2 dolomites demonstrate similar dolomitization fluids related to seawater or marine-origin fluids. D3 dolomites are interpreted to be hydrothermal-derived, which exhibit a different REE partition pattern by contrast. The negative Eu anomalies of D3 dolomites may represent hydrothermal fluid-cooling or the association with intermediate-felsic igneous rocks.

DATA AVAILABILITY STATEMENT

The original contributions presented in the study are included in the article/Supplementary Material; further inquiries can be directed to the corresponding author.

AUTHOR CONTRIBUTIONS

JL: conceptualization and original draft; SL and CM: supervision and project administration; LL and XL: data curation and visualization; JD: investigation and review and editing.

FUNDING

This work is funded by the Key Laboratory of Sedimentary Basin and Oil and Gas Resources (Ministry of Natural Resources, China) (Grant No. cdcgs2020005).

SUPPLEMENTARY MATERIAL

The Supplementary Material for this article can be found online at: <https://www.frontiersin.org/articles/10.3389/feart.2022.927066/full#supplementary-material>

REFERENCES

- Al-Aasm, I. S. (2000). Chemical and Isotopic Constraints for Recrystallization of Sedimentary Dolomites from the Western Canada Sedimentary Basin. *Aquat. Geochem.* 6 (2), 227–248. doi:10.1023/a:1009611224589
- Al-Aasm, I. S., and Crowe, R. (2018). Fluid Compartmentalization and Dolomitization in the Cambrian and Ordovician Successions of the Huron Domain, Michigan Basin. *Mar. Petroleum Geol.* 92, 160–178. doi:10.1016/j.marpetgeo.2018.02.011
- Al-Aasm, I. S., Lonnee, J., and Clarke, J. (2002). Multiple Fluid Flow Events and the Formation of Saddle Dolomite: Case Studies from the Middle Devonian of the Western Canada Sedimentary Basin. *Mar. Petroleum Geol.* 19 (3), 209–217. doi:10.1016/s0264-8172(02)00013-2
- Alibo, D. S., and Nozaki, Y. (1999). Rare Earth Elements in Seawater: Particle Association, Shale-Normalization, and Ce Oxidation. *Geochimica Cosmochimica Acta* 63 (3-4), 363–372. doi:10.1016/s0016-7037(98)00279-8
- Azmy, K., Lavoie, D., Knight, L., and Chi, G. (2008). Dolomitization of the Lower Ordovician Aguathuna Formation carbonates, Port au Port Peninsula, western Newfoundland, Canada: implications for a hydrocarbon reservoir. *Can. J. Earth Sci.* 45 (7), 795–813. doi:10.1139/e08-020
- Azmy, K., Veizer, J., Misi, A., de Oliveira, T. F., Sanches, A. L., and Dardenne, M. A. (2001). Dolomitization and Isotope Stratigraphy of the Vazante Formation, Sao Francisco Basin, Brazil. *Precambrian Res.* 112 (3-4), 303–329. doi:10.1016/s0301-9268(01)00194-2
- Bau, M., and Dulski, P. (1965). Distribution of Yttrium and Rare-Earth Elements in the Penge and Kuruman Iron-Formations, Transvaal Supergroup, South Africa. *Precambrian Res.* 79 (1-2), 37
- Bau, M. (1991). Rare-earth Element Mobility during Hydrothermal and Metamorphic Fluid-Rock Interaction and the Significance of the Oxidation State of Europium. *Chem. Geol.* 93 (3-4), 219–230. doi:10.1016/0009-2541(91)90115-8
- Brand, U., and Veizer, J. (1980). Chemical Diagenesis of a Multicomponent Carbonate System; 1, Trace Elements. *J. Sediment. Petrology* 50 (4), 1219–1236. doi:10.1306/212f7bb7-2b24-11d7-8648000102c1865d
- Budd, D. A. (1997). Cenozoic Dolomites of Carbonate Islands: Their Attributes and Origin. *Earth-Science Rev.* 42, 1–47. doi:10.1016/s0012-8252(96)00051-7

- Chow, N., and James, N. P. (1992). Bulletin of Canadian Petroleum Geology. *Geol. Soc. Am. Bull.* 40 (2), 115
- Davies, G. R., and Smith, L. B. (2006). Structurally Controlled Hydrothermal Dolomite Reservoir Facies: An Overview. *Bulletin* 90 (11), 1641–1690. doi:10.1306/05220605164
- Dickson, J. A. D. (1965). A Modified Staining Technique for Carbonates in Thin Section. *Nature* 205, 587. doi:10.1038/205587a0
- Douville, E., Charlou, J. L., Oelkers, E. H., Bienvenu, P., Colon, C. F. J., Donval, J. P., et al. (2002). The Rainbow Vent Fluids (36 Degrees 14 ' N, MAR): the Influence of Ultramafic Rocks and Phase Separation on Trace Metal Content in Mid-Atlantic Ridge Hydrothermal Fluids. *Chem. Geol.* 184 (1-2), 37–48. doi:10.1016/s0009-2541(01)00351-5
- Du, Y., Fan, T., Machel, H. G., and Gao, Z. (2018). Genesis of Upper Cambrian-Lower Ordovician Dolomites in the Tahe Oilfield, Tarim Basin, NW China: Several Limitations from Petrology, Geochemistry, and Fluid Inclusions. *Mar. Petroleum Geol.* 91, 43–70. doi:10.1016/j.marpetgeo.2017.12.023
- Feng, F., Guan, P., Liu, W. H., Zhang, W., Liu, P. X., Jian, X., et al. (2016). Geochemistry of Altungol Cap Dolostones from the Tarim Basin, NW China. *Arabian J. Geosciences* 9 (17), 1–14. doi:10.1007/s12517-016-2734-x
- Friedman, G. M. (2007). Structurally Controlled Hydrothermal Dolomite Reservoir Facies: An Overview: Discussion. *Bulletin* 91 (9), 1339–1341. doi:10.1306/04300706142
- Guo, R., Zhang, S., Wang, K., Han, M., and Ding, X. (2021). Multiphase Dolomitization and Hydrothermal Alteration of the Upper Cambrian-Lower Ordovician Carbonates in the Gucheng Uplift, Tarim Basin (NW China). *J. Petroleum Sci. Eng.* 206, 108964. doi:10.1016/j.petrol.2021.108964
- Guo, Z. W., Deng, K. L., and Han, Y. H. (1996). *The Formation and Evolution of Sichuan Basin*. Beijing: Geological Publishing House. (in Chinese).
- Haas, J. R., Shock, E. L., and Sassani, D. C. (1995). Rare Earth Elements in Hydrothermal Systems: Estimates of Standard Partial Molal Thermodynamic Properties of Aqueous Complexes of the Rare Earth Elements at High Pressures and Temperatures. *Geochimica Cosmochimica Acta* 59 (21), 4329–4350. doi:10.1016/0016-7037(95)00314-p
- Hein, J. R., Gray, S. C., Richmond, B. M., and White, L. D. (1992). Dolomitization of Quaternary Reef Limestone, Aitutaki, Cook Islands. *Sedimentology* 39 (4), 645–661. doi:10.1111/j.1365-3091.1992.tb02142.x
- Hollis, C., Bastesen, E., Boyce, A., Corlett, H., Gawthorpe, R., Hirani, J., et al. (2017). Fault-controlled Dolomitization in a Rift Basin. *Geology* 45 (3), 219–222. doi:10.1130/g38s394.1
- Hou, M. C., Jiang, W. J., Xing, F. C., Xu, S. L., Liu, X. C., and Xiao, C. (2016a). Origin of Dolomites in the Cambrian (Upper 3rd-Furongian) Formation, South-eastern Sichuan Basin, China. *Geofluids* 16 (5), 856–876. doi:10.1111/gfl.12193
- Hou, Y., Azmy, K., Berra, F., Jadoul, F., Blamey, N. J. F., Gleeson, S. A., et al. (2016b). Origin of the Breno and Esino Dolomites in the Western Southern Alps (Italy): Implications for a Volcanic Influence. *Mar. Petroleum Geol.* 69, 38–52. doi:10.1016/j.marpetgeo.2015.10.010
- Jiang, W. J., Hou, M. C., Xing, F. C., Xu, S. L., and Lin, L. (2016). Characteristics and Indications of Rare Earth Elements in Dolomite of the Cambrian Loushanguan Group SE Sichuan Basin. *Oil Gas Geol.* 37 (4), 473–482. doi:10.11743/ogg20160403
- Jiang, Y., Tan, X., Zhang, C., Jiang, W., Wang, J., Luo, L., et al. (2021). Genesis of Dolomite in Middle Permian Maokou Formation in Eastern Sichuan: Constraints from *In Situ* Geochemistry, Sr-Mg Isotopes, and Fluid Inclusions. *Geofluids* 2021, 1–22. doi:10.1155/2021/6611140
- Jiu, B., Huang, W., Mu, N., and He, M. (2020). Effect of Hydrothermal Fluids on the Ultra-deep Ordovician Carbonate Rocks in Tarim Basin, China. *J. Petroleum Sci. Eng.* 194, 107445. doi:10.1016/j.petrol.2020.107445
- Kareem, K. H., Al-Aasm, I. S., and Mansurbeg, H. (2021). Geochemical Constraints of Hydrothermal Alteration of Dolostones: An Example of Lower Cretaceous Qamchuqa Formation, Kurdistan Region, Northern Iraq. *Mar. Petroleum Geol.* 134, 105337. doi:10.1016/j.marpetgeo.2021.105337
- Kawabe, I., Toriumi, T., Ohta, A., and Miura, N. (1998). Monoisotopic REE Abundances in Seawater and the Origin of Seawater Tetrad Effect. *Geochem. J.* 32 (4), 213–229. doi:10.2343/geochemj.32.213
- Land, L. S. (1985). The Origin of Massive Dolomite. *J. Geol. Educ.* 33 (2), 112–125. doi:10.5408/0022-1368-33.2.112
- Lei, H. J., Li, G. R., Gao, Y. W., Zhou, J. L., Feng, Y. Y., Fu, H., et al. (2016). Geochemical Characteristics and Generation Mechanism of Cambrian Dolomite in the South of Sichuan Basin. *Mar. Orig. Pet. Geol.* 21 (3), 39–47. doi:10.3969/j.issn.1672-9854.2016.03.005
- Li, G. R., Liu, Z. Z., Xie, Z. X., Duan, Y. M., He, S., Deng, M. Z., et al. (2020). Discovery of Non-hydrothermal Saddle-Shaped Dolomite in Leikoupo Formation, Western Sichuan Basin and its Significance. *Oil Gas Geol.* 41 (1), 164. doi:10.11743/ogg20200115
- Li, T., Zhu, D., Yang, M., Zhang, X., Li, P., Lu, C., et al. (2021). Early-stage Marine Dolomite Altered by Hydrothermal Fluids in the Middle Permian Maokou Formation in the Eastern Sichuan Basin, Southern China. *Mar. Petroleum Geol.* 134, 105367. doi:10.1016/j.marpetgeo.2021.105367
- Li, W., Fan, R., Jia, P., Lu, Y., Zhang, Z., Li, X., et al. (2019). Sequence Stratigraphy and Lithofacies Paleogeography of the Middle-Upper Cambrian Xixiangchi Group in the Sichuan Basin and its Adjacent Area, SW China. *Petroleum Explor. Dev.* 46 (2), 238–252. doi:10.1016/s1876-3804(19)60005-4
- Luczaj, J. A., Harrison, W. B., and Smith Williams, N. (2006). Fractured Hydrothermal Dolomite Reservoirs in the Devonian Dundee Formation of the Central Michigan Basin. *Bulletin* 90 (11), 1787–1801. doi:10.1306/06270605082
- Machel, H. G. (2004). “Concepts and Models of Dolomitization: a Critical Reappraisal.” in *The Geometry and Petrogenesis of Dolomite Hydrocarbon Reservoirs*. Editors C. J. R. Braithwaite, G. Rizzi, and G. Darke (the Geological Society of London), 235, 7–63. doi:10.1144/gsl.sp.2004.235.01.02
- Machel, H. G., and Lonnee, J. (2002). Hydrothermal Dolomite - a Product of Poor Definition and Imagination. *Sediment. Geol.* 152 (3-4), 163–171. doi:10.1016/s0037-0738(02)00259-2
- Mahboubi, A., Nowrouzi, Z., Al-Aasm, I. S., Moussavi-Harami, R., and Mahmudy-Gharai, M. H. (2016). Dolomitization of the Silurian Niur Formation, Tabas Block, East Central Iran: Fluid Flow and Dolomite Evolution. *Mar. Petroleum Geol.* 77, 791–805. doi:10.1016/j.marpetgeo.2016.07.023
- Malone, M. J., and Paul, A. (1996). Hydrothermal Dolomitization and Recrystallization of Dolomite Breccias from the Miocene Monterey Formation, Tepusquet Area, California. *J. Sediment. Petrology* 66 (5), 976–990. doi:10.1306/d426845a-2b26-11d7-8648000102c1865d
- Mansurbeg, H., Alsuwaidi, M., Salih, N., Shahrokhi, S., and Morad, S. (2021). Integration of Stable Isotopes, Radiometric Dating and Microthermometry of Saddle Dolomite and Host Dolostones (Cretaceous Carbonates, Kurdistan, Iraq): New Insights into Hydrothermal Dolomitization. *Mar. Petroleum Geol.* 127, 104989. doi:10.1016/j.marpetgeo.2021.104989
- McLennan, S. M. (1989). Chapter 7. Rare Earth Elements in Sedimentary Rocks: Influence of Provenance and Sedimentary Processes. *Rev. Mineralogy Geochem.* 21 (1), 169–200. doi:10.1515/9781501509032-010
- Montanez, I. P. (1994). Late Diagenetic Dolomitization of Lower Ordovician Upper Knox Carbonates: A Record of the Hydrodynamic Evolution of the Southern Appalachian Basin. *AAPG Bull.* 78 (8), 1210–1239. doi:10.1306/a25feb3-171b-11d7-8645000102c1865d
- Montanez, I. P., Osleger, D. A., Banner, J. L., and Mack, L. E. M., M. (2000). Evolution of the Sr and C Isotope Composition of Cambrian Oceans. *GSA Today* 10, 1–7.
- Morad, S., Al-Aasm, I. S., Nader, F. H., Ceriani, A., Gasparrini, M., and Mansurbeg, H. (2012). Impact of Diagenesis on the Spatial and Temporal Distribution of Reservoir Quality in the Jurassic Arab D and C Members, Offshore Abu Dhabi Oilfield, United Arab Emirates. *Geoarabia* 17 (3), 17–56. doi:10.2113/geoarabia170317
- Murphy, A. E., Wieman, S. T., Gross, J., Stern, J. C., Steele, A., and Glamoclija, M. (2020). Preservation of Organic Carbon in Dolomitized Cambrian Stromatolites and Implications for Microbial Biosignatures in Diagenetically Replaced Carbonate Rock. *Sediment. Geol.* 410, 10577. doi:10.1016/j.sedgeo.2020.105777
- Ning, M., Lang, X., Huang, K., Li, C., Huang, T., Yuan, H., et al. (2020). Towards Understanding the Origin of Massive Dolostones. *Earth Planet. Sci. Lett.* 545, 116403. doi:10.1016/j.epsl.2020.116403
- Pan, L., Hu, A., Liang, F., Jiang, L., Hao, Y., Feng, Y., et al. (2021). Diagenetic Conditions and Geodynamic Setting of the Middle Permian Hydrothermal Dolomites from Southwest Sichuan Basin, SW China: Insights from *In Situ* U-Pb Carbonate Geochronology and Isotope Geochemistry. *Mar. Petroleum Geol.* 129, 105080. doi:10.1016/j.marpetgeo.2021.105080

- Peng, B., Li, G., Li, Z., Liu, C., Zuo, Y., Zhang, W., et al. (2018). Discussion of Multiple Formation Mechanisms of Saddle Dolomites-Comparison of Geochemical Data of Proterozoic-Paleozoic Dolomites. *Energy Explor. Exploitation* 36 (1), 66–96. doi:10.1177/0144598717728464
- Rieger, P., Magnall, J. M., Gleeson, S. A., Oelze, M., Wilke, F. D. H., and Lilly, R. (2022). Differentiating between Hydrothermal and Diagenetic Carbonate Using Rare Earth Element and Yttrium (REE+Y) Geochemistry: a Case Study from the Paleoproterozoic George Fisher Massive Sulfide Zn Deposit, Mount Isa, Australia. *Min. Deposita* 57 (2), 187–206. doi:10.1007/s00126-021-01056-1
- Salih, N., Mansurbeg, H., Kolo, K., Gerdes, A., and Pr at, A. (2020). *In Situ* U-Pb Dating of Hydrothermal Diagenesis in Tectonically Controlled Fracturing in the Upper Cretaceous Bekhme Formation, Kurdistan Region-Iraq. *Int. Geol. Rev.* 62 (18), 2261–2279. doi:10.1080/00206814.2019.1695151
- Shembilu, N., Azmy, K., and Blamey, N. (2021). Origin of Middle-Upper Cambrian Dolomites in Eastern Laurentia: A Case Study from Belle Isle Strait, Western Newfoundland. *Mar. Petroleum Geol.* 125, 104858. doi:10.1016/j.marpetgeo.2020.104858
- Smith, L. B. (2006). Origin and Reservoir Characteristics of Upper Ordovician Trenton-Black River Hydrothermal Dolomite Reservoirs in New York. *AAPG Bull.* 90 (11), 1787–1801. doi:10.1306/04260605078
- Su, A., Chen, H., Feng, Y.-x., Zhao, J.-x., Wang, Z., Hu, M., et al. (2022). *In Situ* U-Pb Dating and Geochemical Characterization of Multi-Stage Dolomite Cementation in the Ediacaran Dengying Formation, Central Sichuan Basin, China: Constraints on Diagenetic, Hydrothermal and Paleo-Oil Filling Events. *Precambrian Res.* 368, 106481. doi:10.1016/j.precamres.2021.106481
- Tortola, M., Al-Aasm, I. S., and Crowe, R. (2020). Diagenetic Pore Fluid Evolution and Dolomitization of the Silurian and Devonian Carbonates, Huron Domain of Southwestern Ontario: Petrographic, Geochemical and Fluid Inclusion Evidence. *Minerals* 10 (2), 140. doi:10.3390/min10020140
- Veizer, J., Ala, D., Azmy, K., Bruckschen, P., Buhl, D., Bruhn, F., et al. (1999). 87Sr/86Sr, d13C and d18O Evolution of Phanerozoic Seawater. *Chem. Geol.* 161 (1–3), 59–88. doi:10.1016/s0009-2541(99)00081-9
- Veizer, J. (1983). “Chemical Diagenesis of Carbonates: Theory and Application of Trace Element Technique,” in *Stable Isotopes in Sedimentary Geology*. Editors M. A. Arthur, T. F. Anderson, I. R. Kaplan, J. Veizer, and L. S. Land (Dallas, United States: Society of Economic Paleontologists and Mineralogists Short Course Notes 10, 1–100.
- Wang, S.-f., Li, W., Zhang, F., and Wang, X.-z. (2008). Developmental Mechanism of Advantageous Xixiangchi Group Reservoirs in Leshan-Longnusi Palaeohigh. *Petroleum Explor. Dev.* 35 (2), 170–174. doi:10.1016/s1876-3804(08)60023-3
- Warren, J. (2000). Dolomite: Occurrence, Evolution and Economically Important Associations. *Earth-Science Rev.* 52 (1–3), 1–81. doi:10.1016/s0012-8252(00)00022-2
- Yang, X., Huang, Z., Wang, X., Wang, Y., Li, K., and Zeng, D. (2019). Origin of Crystal Dolomite and its Reservoir Formation Mechanism in the Xixiangchi Formation, Upper Cambrian in Southeastern Sichuan Basin. *Carbonates Evaporites* 34 (4), 1537–1549. doi:10.1007/s13146-019-00499-y
- Yang, X., Mei, Q., Wang, X., Dong, Z., Li, Y., and Huo, F. (2018). Indication of Rare Earth Element Characteristics to Dolomite Petrogenesis-A Case Study of the Fifth Member of Ordovician Majiagou Formation in the Ordos Basin, Central China. *Mar. Petroleum Geol.* 92, 1028–1040. doi:10.1016/j.marpetgeo.2017.12.004
- Zhai, G. M. (1989). *Petroleum Geology of China*. Beijing: Petroleum Industry Press. (in Chinese).
- Zhang, J., Hu, W., Qian, Y., Wang, X., Cao, J., Zhu, J., et al. (2009). Formation of Saddle Dolomites in Upper Cambrian Carbonates, Western Tarim Basin (Northwest China): Implications for Fault-Related Fluid Flow. *Mar. Petroleum Geol.* 26 (8), 1428–1440. doi:10.1016/j.marpetgeo.2009.04.004
- Zhang, W., Guan, P., Jian, X., Feng, F., and Zou, C. (2014). In Situ Geochemistry of Lower Paleozoic Dolomites in the Northwestern Tarim Basin: Implications for the Nature, Origin, and Evolution of Diagenetic Fluids. *Geophys. Geosyst.* 15 (7), 2744–2764. doi:10.1002/2013gc005194
- Zhao, A. W., Tan, X. C., Li, L., Luo, B., Hong, H. T., Liu, J. W., et al. (2015). Characteristics and Distribution of Grain Banks in the Cambrian Xixiangchi Group of Sichuan Basin and its Adjacent Areas. *J. Palaeogeogr.* 17 (1), 21–32. doi:10.7605/gdxb.2015.01.002
- Zhu, D., Jin, Z., and Hu, W. (2010). Hydrothermal Recrystallization of the Lower Ordovician Dolomite and its Significance to Reservoir in Northern Tarim Basin. *Sci. China Earth Sci.* 53 (3), 368–381. doi:10.1007/s11430-010-0028-9

Conflict of Interest: The authors declare that the research was conducted in the absence of any commercial or financial relationships that could be construed as a potential conflict of interest.

Publisher’s Note: All claims expressed in this article are solely those of the authors and do not necessarily represent those of their affiliated organizations, or those of the publisher, the editors and the reviewers. Any product that may be evaluated in this article, or claim that may be made by its manufacturer, is not guaranteed or endorsed by the publisher.

Copyright © 2022 Liang, Liu, Li, Dai, Li and Mou. This is an open-access article distributed under the terms of the Creative Commons Attribution License (CC BY). The use, distribution or reproduction in other forums is permitted, provided the original author(s) and the copyright owner(s) are credited and that the original publication in this journal is cited, in accordance with accepted academic practice. No use, distribution or reproduction is permitted which does not comply with these terms.